Article

Chinese Science Bulletin

Optics

July 2012 Vol. 57 No. 21: 2747–2751
doi: 10.1007/s11434-012-5243-7

Study of stimulated Raman and Brillouin scattering in a finite interaction region under the convective instability condition

HAO Liang[1*], LIU ZhanJu[1], ZHENG ChunYang[1,2], XIANG Jiang[1], FENG Wu[3], HU XiaoYan[1] & LI Bin[1]

[1] *Institute of Applied Physics and Computational Mathematics, Beijing 100094, China;*
[2] *Center for Applied Physics and Technology, Peking University, Beijing 100871, China;*
[3] *Graduate School of China Academy of Engineering Physics, Beijing 100088, China*

Received December 12, 2011; accepted February 6, 2012

We discuss stimulated Raman scattering (SRS) and stimulated Brillouin scattering (SBS) under the convective instability condition with a one-dimensional three-wave interaction (3WI) model. Using linear theory, we deduce the temporal growth rate, gain exponent, and reflectivity of the backward scattered wave in a finite interaction region. We find that the growth rate is not only determined by the laser intensity and plasma density and temperature, but also related to the spatial gain. The length of the interaction region is important to the gain exponent and backscattering level. We simulate the developments and evolutions of SRS and SBS based on the 3WI equations. Our numerical results consist with the linear theory.

stimulated Raman scattering, stimulated Brillouin scattering, three-wave interaction model

Citation: Hao L, Liu Z J, Zheng C Y, et al. Study of stimulated Raman and Brillouin scattering in a finite interaction region under the convective instability condition. Chin Sci Bull, 2012, 57: 2747–2751, doi: 10.1007/s11434-012-5243-7

Both stimulated Raman scattering (SRS) and stimulated Brillouin scattering (SBS) are central problems in laser-driven inertial confinement fusion (ICF) [1, 2]. When SRS happens, a resonant decay of an incident light wave into a scattered light wave and a Langmuir wave occurs. Similarly, in SBS the incident light wave decays resonantly into a scattered light wave and an ion acoustic wave. The backward scattering processes of SRS and SBS lead to energy loss when the incident laser propagates over underdense plasma, and play crucial roles in laser fusion [3]. SRS and SBS have been widely studied in theory over the past four decades [4–17]. Recently, relevant experiments and techniques have also developed rapidly [18–21]. However, most work so far has mainly concentrated on the relation between the backscattering reflectivity and the plasma density or temperature. Discussions about the effect of the spatial interaction region are lacking. In this work, we study the SRS and SBS process based on a one-dimensional three-wave interaction (3WI) model with a finite plasma under the convective instability condition, and focus on the spatial influence on the backward scattered waves.

*Corresponding author (email: hao_liang@iapcm.ac.cn)

1 Physical model

In this section, we introduce our physical model, which is powerful in large-scale simulation [8]. Firstly, we define $A_0(z,t)$, $A_R(z,t)$ and $A_B(z,t)$ as the slowly varying complex amplitudes of the vector potentials for the incident light, SRS backscattering light, and SBS backscattering light, respectively. ω_0, ω_R, and ω_B are the relevant frequencies. δn_L and δn_A represent the rapidly-varying perturbations of the electron density n_e with the frequencies ω_L and ω_A responsible for SRS and SBS, respectively. Under the linear envelope approximation, the one-dimensional SRS process in homogeneous plasma can be described by the 3WI equations [8]:

$$\left(\frac{\partial}{\partial t}+\nu_0+v_{g0}\frac{\partial}{\partial z}\right)A_0(z,t)=-\frac{i\pi e^2}{m_e\omega_0}\delta n_L(z,t)A_R(z,t), \quad (1)$$

$$\left(\frac{\partial}{\partial t}+\nu_R-v_{gR}\frac{\partial}{\partial z}\right)A_R(z,t)=-\frac{i\pi e^2}{m_e\omega_R}\delta n_L^*(z,t)A_0(z,t), \quad (2)$$

$$\left(\frac{\partial}{\partial t}+\nu_{epw}+v_{gL}\frac{\partial}{\partial z}\right)\delta n_L(z,t)=-\frac{in_e e^2k_L^2}{4\omega_L m_e^2c^2}\left[A_0(z,t)A_R^*(z,t)\right], \quad (3)$$

where $\omega_0=\omega_R+\omega_L$ and $k_0=k_L-k_R$, $k_0=\omega_0/c\sqrt{1-n_e/n_c}$ is the wavenumber of the incident light wave, k_R and k_L denote the wavenumbers of the backscattering light wave and the Langmir wave, $v_{g0}=c^2k_0/\omega_0$, $v_{gR}=c^2k_R/\omega_R$, and $v_{gL}=3T_ek_L/(m_e\omega_L)$ are the group velocities of the three waves, and $\nu_0=\omega_{pe}^2\nu_{ei}/(2\omega_0^2)$, $\nu_R=\omega_{pe}^2\nu_{ei}/(2\omega_R^2)$, and $\nu_{epw}=\omega_{pe}^2\nu_{ei}/(2\omega_L^2)+\nu_{epw}^L$ are the relevant damping rates, respectively. As usual, T_e, m_e, e, c, ω_{pe}, ν_{ei}, and n_c are the electron temperature, electron mass, electron charge, vacuum speed of light, electron plasma frequency, electron-ion collision frequency, and critical density. $\nu_{epw}^L=\sqrt{\pi/8}\omega_L(k_L\lambda_D)^{-3}\exp\left(-\left(\sqrt{2}k_L\lambda_D\right)^{-2}-3/2\right)$ is the Landau damping rate of the Langmir wave.

Similarly, the 3WI equations of one-dimensional SBS are [8]

$$\left(\frac{\partial}{\partial t}+\nu_0+v_{g0}\frac{\partial}{\partial z}\right)A_0(z,t)=-\frac{i\pi e^2}{m_e\omega_0}\delta n_A(z,t)A_B(z,t), \quad (4)$$

$$\left(\frac{\partial}{\partial t}+\nu_0-v_{g0}\frac{\partial}{\partial z}\right)A_B(z,t)=-\frac{i\pi e^2}{m_e\omega_0}\delta n_A^*(z,t)A_0(z,t), \quad (5)$$

$$\left(\frac{\partial}{\partial t}+\nu_{iaw}+C_s\frac{\partial}{\partial z}\right)\delta n_A(z,t)=-\frac{iZn_e e^2k_0}{2m_im_ec^2C_s}\left[A_0(z,t)A_B^*(z,t)\right], \quad (6)$$

where we assume that $\omega_B\approx\omega_0$, $k_B\approx k_0$, $k_A\approx 2k_0$ and $\omega_A\approx 2k_0C_s$ [6–8]. $C_s=\sqrt{(ZT_e+3T_i)/m_i}$ is the isothermal sound speed, Z is the atomic number, m_i is the ion mass, and T_i is the ion temperature. $\nu_{iaw}=\nu_{ie}/2+\nu_{iaw}^L$ is the damping rate of the ion sound wave, where ν_{ie} is the ion-electron collision frequency and $\nu_{iaw}^L=\sqrt{\pi/8}\omega_A\left((Zm_e/m_i)^{1/2}+(ZT_e/T_i)^{3/2}\exp(-ZT_e/(2T_i)-3/2)\right)$ is the Landau damping rate of the ion sound wave.

2 Linear theory

Based on the physical model described above, the temporal growth rate γ, gain exponent G, and reflectivity R of the SRS and SBS backscattering light waves are deduced in detail as follows.

To study the SRS process, eqs. (1)–(3) can be rewritten for simplicity as

$$\left(\frac{\partial}{\partial t}+\nu_0+v_{g0}\frac{\partial}{\partial z}\right)c_0(z,t)=-\frac{v_{g0}\gamma_{0R}}{\sqrt{v_{gL}v_{gR}}}c_L(z,t)c_R(z,t), \quad (7)$$

$$\left(\frac{\partial}{\partial t}+\nu_R-v_{gR}\frac{\partial}{\partial z}\right)c_R(z,t)=\sqrt{\frac{v_{gR}}{v_{gL}}}\gamma_{0R}c_L^*(z,t)c_0(z,t), \quad (8)$$

$$\left(\frac{\partial}{\partial t}+\nu_{epw}+v_{gL}\frac{\partial}{\partial z}\right)c_L(z,t)=\sqrt{\frac{v_{gL}}{v_{gR}}}\gamma_{0R}c_0(z,t)c_R^*(z,t), \quad (9)$$

where $c_0(z,t)=A_0(z,t)/A_0(0,0)$, $c_R(z,t)=\sqrt{k_R/k_0}A_R(z,t)/A_0(0,0)$, and $c_L(z,t)=i\sqrt{v_{gL}/k_0\omega_R}\pi e^2\delta n_L(z,t)/(\gamma_{0R}m_ec)$ are the three normalized complex wave amplitudes. $\gamma_{0R}=\sqrt{\omega_{pe}^2/\omega_R\omega_L}k_LeA(0,0)/(4m_ec)$ is the maximum homogeneous Raman growth rate [6]. Assuming c_0 stays unchanged, if the solution form of c_R and c_L is $\exp(\gamma_Rt+q_Rz)$, where γ_R is the SRS temporal growth rate and q_R is the SRS spatial gain, the dispersion relation

$$\left(\gamma_R+\nu_R-q_Rv_{gR}\right)\left(\gamma_R+\nu_{epw}+q_Rv_{gL}\right)=\gamma_{0R}^2 \quad (10)$$

is obtained from eqs. (8) and (9). Solving eq. (10) for γ_R, we get

$$\gamma_R=\sqrt{\left(\nu_{epw}+q_Rv_{gL}-\nu_R+q_Rv_{gR}\right)^2/4+\gamma_{0R}^2}-\left(\nu_{epw}+q_Rv_{gL}+\nu_R-q_Rv_{gR}\right)/2. \quad (11)$$

From the expression for γ_R, we find that the temporal growth rate is not only determined by the incident light condition and the plasma density and temperature, but also by the spatial gain q_R. Setting $q_R=0$, we obtain

$$\gamma_R=\sqrt{\left(\nu_{epw}-\nu_R\right)^2/4+\gamma_{0R}^2}-\left(\nu_{epw}+\nu_R\right)/2, \quad (12)$$

which is the general expression of γ_R [9]. If the damping rates ν_R and ν_{epw} are neglected, γ_R reaches its maximum γ_{0R}. Note that SRS instability occurs only when $\gamma_R>0$, from which we get the usual SRS threshold $\gamma_{thR}=\sqrt{\nu_{epw}\nu_R}$. Solving eq. (10) for q_R, we obtain

$$q_R=\frac{1}{2}\left\{\left(\frac{\gamma_R+\nu_R}{v_{gR}}-\frac{\gamma_R+\nu_{epw}}{v_{gL}}\right)\pm\sqrt{\left(\frac{\gamma_R+\nu_R}{v_{gR}}+\frac{\gamma_R+\nu_{epw}}{v_{gL}}\right)^2-4\frac{\gamma_{0R}^2}{v_{gL}v_{gR}}}\right\}. \quad (13)$$

Absolute SRS instability happens when the radical of eq. (13) is equal to zero for $\gamma_R>0$, which implies γ_{0R} should be at least larger than $\sqrt{v_{gL}v_{gR}/4}\left(\nu_R/v_{gR}+\nu_{epw}/v_{gL}\right)$ [6]. So the threshold of absolute SRS instability is $\gamma_{AR}=\sqrt{v_{gL}v_{gR}/4}\left(\nu_R/v_{gR}+\nu_{epw}/v_{gL}\right)$, and the condition for convective SRS instability is $\gamma_{thR}<\gamma_{0R}<\gamma_{AR}$ [5,6].

We now get the backscattering reflectivity of SRS under the convective condition after it evolves into the stable state. Considering the common case $\nu_{epw}\gg\nu_R$, $\nu_{epw}\gg\nu_0$, eqs. (7)–(9) are simplified as

$$\frac{\partial}{\partial z}c_0(z)=-\frac{\gamma_{0R}}{\sqrt{v_{gL}v_{gR}}}c_L(z)c_R(z), \quad (14)$$

$$\frac{\partial}{\partial z}c_R(z)=-\frac{\gamma_{0R}}{\sqrt{v_{gL}v_{gR}}}c_L^*(z)c_0(z), \quad (15)$$

$$\left(\frac{\nu_{epw}}{v_{gL}}+\frac{\partial}{\partial z}\right)c_L(z)=\frac{\gamma_{0R}}{\sqrt{v_{gL}v_{gR}}}c_0(z)c_R^*(z). \quad (16)$$

Integrating eq. (16) under some reasonable approximations,

$$c_L(z)\approx\frac{\gamma_{0R}}{\sqrt{v_{gL}v_{gR}}}\frac{v_{gL}}{\nu_{epw}}c_0(z)c_R^*(z), \quad (17)$$

is obtained [4]. Substituting eq. (17) into eqs. (15) and (16) leads to

$$\frac{\partial |c_0(z)|^2}{\partial z} = -\frac{2\gamma_{0R}^2}{v_{gR}\nu_{epw}} |c_0(z)|^2 |c_R(z)|^2 , \tag{18}$$

$$\frac{\partial |c_R(z)|^2}{\partial z} = -\frac{2\gamma_{0R}^2}{v_{gR}\nu_{epw}} |c_R(z)|^2 |c_0(z)|^2 . \tag{19}$$

Supposing the length of the interaction region is L, solutions of eqs. (18) and (19) are

$$R(1-R) = \epsilon \{\exp[G_R(1-R)] - R\}, \tag{20}$$

where $R = |c_R(0)|^2$ is the reflectivity, and $\epsilon = |c_R(L)|^2$ is the boundary condition of the backscattering light wave corresponding to the thermal noise. The SRS gain exponent is

$$G_R = \frac{2\gamma_{0R}^2 L}{\nu_{epw} v_{gR}} = \frac{k_L^2 v_{os}^2 \omega_{pe}^2 L}{8\nu_{epw} v_{gR} \omega_R \omega_L}, \tag{21}$$

where $v_{os} = eA_0/(m_e c)$ is the electron quiver velocity.

The SBS process can be discussed in the same way as above, and the theoretical solutions are similar. From eqs. (4)–(6) we obtain the SBS temporal growth rate γ_B as

$$\gamma_B = \sqrt{\left(\nu_{iaw} + q_B C_s - \nu_0 + q_B v_{g0}\right)^2/4 + \gamma_{0B}^2} - \left(\nu_{iaw} + q_B v_{g0} + \nu_0 - q_B v_{g0}\right)/2, \tag{22}$$

where $\gamma_{0B} = \sqrt{Z\omega_{pe}^2/8m_e m_i \omega_0 k_0 C_s} k_0 e A_0(0,0)/c$ is the maximum homogeneous Brillouin growth rate, and q_B is the SBS spatial gain. The reflectivity of the SBS backscattering light wave also satisfies eq. (20) with the replacement $G_B \to G_R$, where the SBS gain exponent is

$$G_B = \frac{2\gamma_{0B}^2 L}{\nu_{iaw} v_{g0}} = \frac{k_A^2 v_{os}^2 \omega_{pi}^2 L}{8\nu_{iaw} v_{g0} \omega_0 \omega_A}, \tag{23}$$

and $\omega_{pi} = \sqrt{Zm_e/m_i}\omega_{pe}$.

3 Simulation results

We have simulated the evolutions of SRS and SBS in a bounded homogeneous plasma under the convective instability condition. The wavelength of incident light is assumed to be $\lambda_c = 0.351\,\mu$m. The electron density is chosen to be $n_e = 0.11 n_c$. The temperatures of electrons and ions are $T_e = 2.5$ keV and $T_i = 0.5$ keV.

Figure 1 shows the SRS reflectivity at $z = 0$ as a function of time with increasing incident laser intensity from 2×10^{15} W/cm^2 to 4.5×10^{15} W/cm^2 corresponding to γ_{0R} from $0.021/\tau_c$ to $0.032/\tau_c$. γ_{thR} and γ_{AR} are calculated to be $0.0012/\tau_c$ and $0.11/\tau_c$, respectively. So the convective SRS instability condition mentioned above is satisfied. The simulated plasma length is $L = 800\lambda_c$. For simplicity, the laser intensity is denoted as $I15$ in the figure legend; for example, $I = 2\times10^{15}$ W/cm^2 is denoted as $I15 = 2$. The amplified subgraph shows the linear growth phase of SRS, and the slopes of the curves stand for different temporal growth rates. It is shown that both the reflectivity and the temporal growth rate of SRS rise when the laser intensity rises. Figure 2 shows the value of $|A_R|^2$ as a function of position at $t = 1000\tau_c$, where the spatial gain q_R is revealed by the slope of the curve. The curves become more and more steep when $I15$ increases. In Figure 3, we give the temporal growth rate and spatial gain as functions of incident laser intensity. Our simulation results for γ_R and q_R are the starred line and short dashed line with black dot, respectively. The long dashed line shows the theoretical value of γ_{0R}. The chain dotted line is calculated from eq. (12), which is the theoretical temporal growth rate neglecting the spatial gain. We substitute the values of q_R into eq. (11) and get the γ_R of linear theory revised with q_R, which is shown as the solid line. We find that the simulated γ_R changes in accord with the revised theoretical one, and both are much smaller than the values calculated from eq. (12). So the spatial gain q_R has visible influence on the temporal growth rate γ_R.

According to the linear theory, the reflectivity in both SRS and SBS is decided by the thermal noise ϵ and the exponent gain G, which is proportional to the incident laser intensity I and plasma length L. So the higher laser intensity and longer plasma length lead to larger reflectivity. Here, the effects of increasing I, L, and ϵ on the reflectivity of SRS and SBS are simulated in turn. The simulation conditions are $\lambda_c = 0.351\,\mu$m, $n_e = 0.11 n_c$, $T_e = 2.5$ keV, $T_i = 0.5$ keV, $Z = 1$, and $m_i = 1836 m_e$. In Figure 4(a) and (b), the reflectivity of SRS and SBS are given as functions of incident laser intensity I, where the plasma length is kept at $L = 800\lambda_c$, and the thermal noise is assumed to be 10^{-9}. The incident laser intensity is still chosen from 2×10^{15} W/cm^2 to 4.5×10^{15} W/cm^2 to satisfy the convective conditions. Figure 4(c) and (d) show a strong dependency of the SRS and SBS

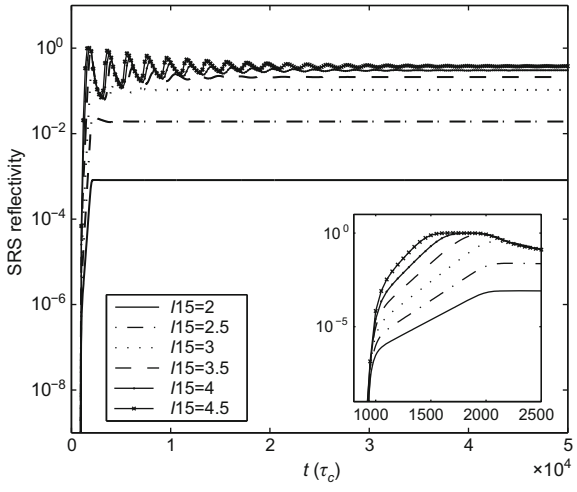

Figure 1 The SRS reflectivity at $z = 0$ varies with time, where τ_c is the laser period in vacuum.

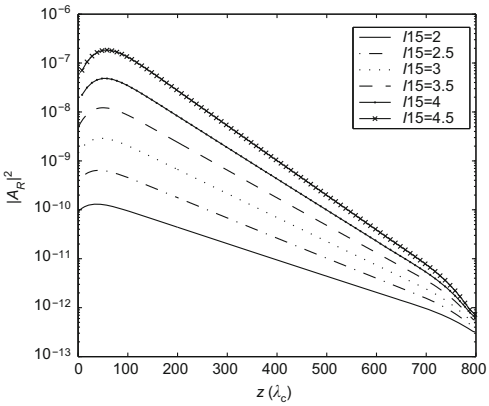

Figure 2 Spatial profile of the SRS light intensity (in dimensionless unit $m_e^2c^4/e^2$) at $t = 1000\tau_c$.

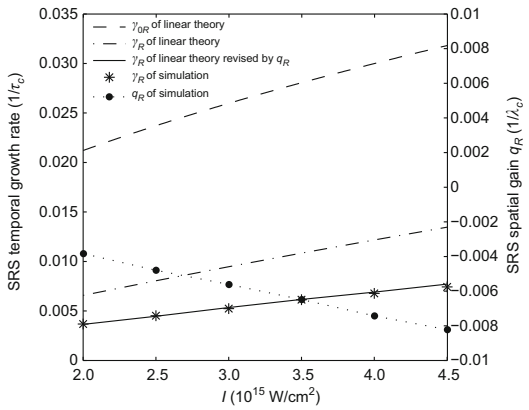

Figure 3 Temporal growth rate and spatial gain as functions of incident laser intensity.

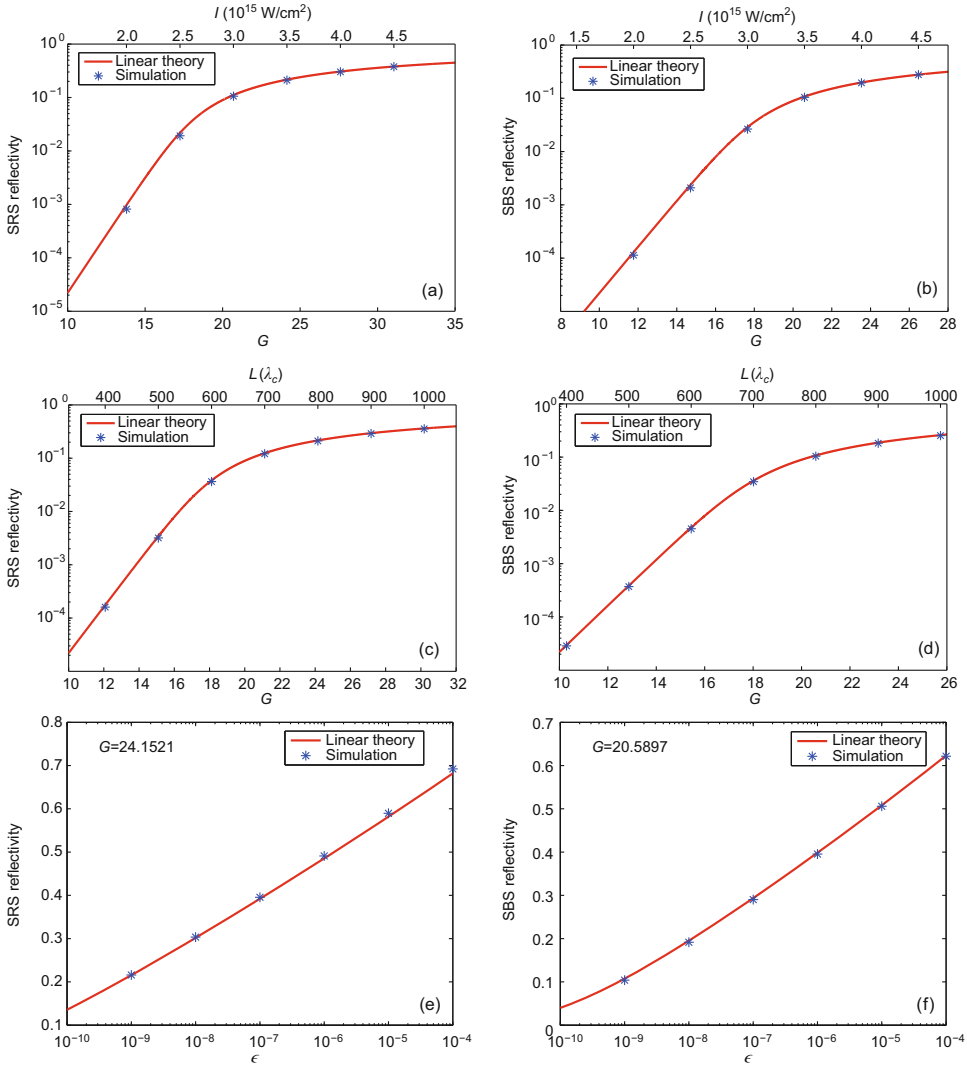

Figure 4 (a) SRS reflectivity varies with the incident laser intensity I and the exponent gain G_R, for $L = 800\lambda_c$ and $\epsilon = 10^{-9}$. (b) SBS reflectivity varies with the incident laser intensity I and the exponent gain G_B, for $L = 800\lambda_c$ and $\epsilon = 10^{-9}$. (c) SRS reflectivity varies with the plasma length L and exponent gain G_R, for $I = 3.5 \times 10^{15}$ W/cm^2 and $\epsilon = 10^{-9}$. (d) SBS reflectivity varies with the plasma length L and exponent gain G_B, for $I = 3.5 \times 10^{15}$ W/cm^2 and $\epsilon = 10^{-9}$. (e) SRS reflectivity varies with ϵ for $I = 3.5 \times 10^{15}$ W/cm^2 and $L = 800\lambda_c$. (f) SBS reflectivity varies with ϵ for $I = 3.5 \times 10^{15}$ W/cm^2 and $L = 800\lambda_c$.

reflectivity on the plasma length, where the incident laser intensity is kept at 3.5×10^{15} W/cm^2 and ϵ is set to be 10^{-9}. At last, the reflectivity of SRS and SBS are simulated as functions of ϵ shown in Figure 4(e) and (f), respectively, where $I = 3.5\times10^{15}$ W/cm^2 and $L = 800\lambda_c$. In these figures, our simulation results are the starred lines, and the theoretical values calculated from the linear theory are the solid curves. Excitedly, the simulation results are almost consistent with the linear theory, which shows the usefulness of the one-dimensional 3WI model and our simulation procedures.

4 Conclusions

We have discussed SRS and SBS under the convective instability condition with a one-dimensional 3WI model. Theoretically, expressions of the temporal growth rate, spatial gain, gain exponent, and reflectivity of the backscattering wave are deduced with the linear approximation by considering a bounded homogeneous plasma. We simulated the evolutions of SRS and SBS and showed that the temporal growth rate is correlated with the spatial gain. Both the incident laser intensity and plasma length are proportional to the gain exponent, which determines the reflectivity of backscatter. The thermal noise is also important to the reflectivity. Our numerical results almost agree with the linear theory, which indicates the practicability of our simulation procedures.

This work was supported by Science and Technology Funds of CAEP (2010B0102018 and 2010A0102004), and the National Natural Science Foundation of China (11147141, 11175029, 11075025, 10975023, 10935003).

1 Kruer W L. The Physics of Laser Plasma Interactions. Redwood City, CA: Addison-Wesley Publishing Co., 1988
2 Lindl J D. Development of the indirect-drive approach to inertial confinement fusion and the target physics basis for ignition and gain. Phys Plasmas, 1995, 2: 3933–4024
3 Powers L V, Berger R L, Kauffman R L, et al. Gas-filled targets for large scale-length plasma interaction experiments on Nova. Phys Plasmas, 1995, 2: 2473–2479
4 Tang C L. Saturation and spectral characteristics of the Stokes emission in the stimulated Brillouin process. J Appl Phys, 1966, 37: 2945–2955
5 Pesme D, Laval G, Pellat R. Parametric instabilities in bounded plasmas. Phys Rev Lett, 1973, 31: 203–206
6 Forslund D W, Kindel J M, Lindman E L. Theory of stimulated scattering processes in laser-irradiated plasmas. Phys Fluids, 1975, 18: 1002–1016
7 Ramani A, Max C E. Stimulated Brillouin scattering in an inhomogeneous plasma with broad-bandwidth thermal noise. Phys Fluids, 1983, 26: 1079–1102
8 Berger R L, Still C H, Williams E A, et al. On the dominant and subdominant behavior of stimulated Raman and Brillouin scattering driven by nonuniform laser beams. Phys Plasmas, 1998, 5 : 4337–4356
9 Boyd T J M, Sanderson J J. The Physics of Plasmas. Cambridge: Cambridge University Press, 2003
10 Hu Y M, Hu X W. Parametric processes of a strong laser in partially ionized plasmas. Phys Rev E, 2003, 67: 036402–036410
11 Lindl J D, Amendt P, Berger R L, et al. The physics basis for ignition using indirect-drive targets on the National Ignition Facility. Phys Plasmas, 2004, 11: 339–491
12 Liu Z J, He X T, Zheng C Y, et al. Excitation of coherent terahertz radiation by stimulated Raman scatterings. Phys Plasmas, 2010, 17: 024502–024504
13 Liu Z J, Zheng C Y, He X T, et al. Stimulated backward Brillouin scattering in two ion-species plasmas. Phys Plasmas, 2011, 18: 032705–032708
14 Zhang Z H, Zhang H A. Explanation of multi-process competition for SRS gain anomaly. Chin Sci Bull, 1993, 38: 111–115
15 Xing L, Zhan L, Xia Y X. Large delay tunable slow-light based on high-gain stimulated-Brillouin-scattering amplification in optical fibers. Chin Sci Bull, 2009, 54: 3947–3952
16 Hasi W, Lu Z W, Li Q, et al. Study on two-cell stimulated Brillouin scattering system with mixture medium . Sci China Ser G-Phys Mech Astron, 2007, 50: 144–151
17 Meng Z W, Sun X P, Fang W H, et al. Influence of amplified spontaneous emission and fluorescence of β-carotene on stimulated Raman scattering of carbon disulfide. Sci China Ser G-Phys Mech Astron, 2009, 52: 529–533
18 Froula D H, Divol L, Meezan N B, et al. Ideal laser-beam propagation through high-temperature ignition Hohlraum plasmas. Phys Rev Lett, 2007, 98: 085001–085004
19 Divol L, Berger R L, Meezan N B, et al. Three-dimensional modeling of laser-plasma interaction: Benchmarking our predictive modeling tools versus experiments. Phys Plasmas, 2008, 15: 056313–056319
20 Michel D T, Depierreux S, Stenz C, et al. Exploring the saturation levels of stimulated Raman scattering in the absolute regime. Phys Rev Lett, 2010, 104: 255001–255004
21 Li Z C, Zheng J, Ding Y K, et al. Generation and characterization of millimeter-scale plasmas for the research of laser plasma interactions on Shenguang-III prototype. Chin Phys B, 2010, 19: 125202